Dual color bioluminescent sensor proteins for therapeutic drug monitoring of anti-tumor antibodies.

Martijn van Rosmalen, Yan Ni, Daan F.M. Vervoort, Remco Arts, Susann K.J. Ludwig, and Maarten Merkx*

Laboratory of Chemical Biology and Institute for Complex Molecular Systems (ICMS), Department of Biomedical Engineering, Eindhoven University of Technology, P.O. Box 513, 5600 MB Eindhoven, the Netherlands.

Supplementary Information

Contents

Supplementary Experimental Procedures

Molecular Cloning

Restriction enzymes, polymerases, ligases and associated reaction buffers were all obtained from New England Biolabs (NEB). pET-28a(+)-CTX-LUMABS-2 (cloned between *NheI* and *NotI*) and pUC-57 vectors containing the linker regions (including epitopes, mimotopes or paratopes) of CTX-Linker-1 and 3, TRAS-Linker-1, 2 and 3, and CD20-Linker-1 were ordered from GenScript (Piscataway, New Jersey, U.S.A.). pET-28a(+)-CTX-LUMABS-1 and 3, and TRAS-LUMABS-1 were made by digesting 1 µg of the pUC-57 vectors with the respective linker regions as well as 1 µg of pET-28a(+)-CTX-LUMABS-2 with 20 units of both *KpnI-HF* and *SpeI-HF* in CutSmart Buffer at 37 °C for 1 hour. Linearized fragments were isolated by agarose gel electrophoresis and purified using the QIAquick Gel Extraction kit (QIAGEN), according to the manufacturer's instructions. 50 ng of the linearized pET-28a(+)-LUMABS and 6 ng of the respective digested linkers (a molar vector : insert ratio of ca. 1 : 5) were then ligated using 400 units of T4 DNA ligase in the supplied buffer at 16 °C for 30 minutes in a reaction volume of 20 µL. One or 2 µL of the ligation was transformed into NovaBlue bacteria (Merck, Novagen) DNA was isolated from single clonal colonies using the QIAquick Miniprep kit (QIAGEN) and DNA was sequenced by StarSEQ GmbH (Mainz, Germany). pET-28a(+)-TRAS-LUMABS-2 was made by cloning a Strep-Tag-II at the C-terminus of TRAS-LUMABS-1 using Multiple Site Directed Mutagenesis as described elsewhere,[1] and subsequently exchanging the linker using restriction / ligation with *KpnI-HF* and *SpeI-HF* as described above. Constructs pET-28a(+)-TRAS-LUMABS 3 and pET-28a(+)-CD20-LUMABS-1 were obtained from pET-28a(+)-TRAS-LUMABS-2 by exchanging the linker region using restriction / ligation with *KpnI-HF* and *SpeI-HF* as described above, while pET-28a(+)-CD20-LUMABS-2 was obtained from pET-28a(+)-CD20-LUMABS-1 using Multiple Site Directed Mutagenesis as described elsewhere.[1] Correct sequences of all sensors described in this study were verified by Sanger sequencing. For Sequences of sensor proteins used in this study, see Supplementary Figures S14 and S15.

Protein Expression and Purification

Protein expression in *E. coli* was essentially done as previously described[2] by inducing exponentially growing BL21(DE3) cells (at an OD_{600} of 0.6) with 0.1 mM IPTG at 25 °C for 16-20 hours. Purification was done by immobilized metal affinity chromatography as described. TRAS-LUMABS-2, 3 and CD20-LUMABS-1 were further purified by Strep-tactin affinity chromatography as described. CTX-LUMABS 1 and 2 were further purified by Size Exclusion Chromatography (SEC) over a 26/60 HiLoad Superdex column with a volume of 300 mL in a buffer containing 50 mM Na_2HPO_4 / NaH_2PO_4 (pH 7.5), 150 mM NaCl, 10% (v/v) glycerol, 1 mM EDTA, and 0.1% (v/v) Triton-X100. All proteins were frozen in liquid nitrogen and stored at -80 °C.

Peptide synthesis.

All peptides with N-terminal fluorescein groups were synthesized using Fmoc-protected solid phase peptide synthesis and labeled at the N-termini with fluorescein iso-thiocyanate via a (5-amino)-3-oxapentanoic acid (O1PEN) linker as described.[3]

Fluorescence Polarization measurements.

For fluorescence polarization assays, peptides were dissolved in dimethylsulfoxide (DMSO) and then diluted to a concentration of 30 nM in PBS pH 7.4 with varying antibody concentrations. Assays were performed in Corning black round-bottom low-volume 384 well microtiter plates in a total volume of 10 µL. Polarization was measured on a Tecan Infinite F500 plate reader using an excitation wavelength of 485 nm an emission wavelength of 535 nm. Through FP data, a one-site binding function of the form of equation 1 (in the main text) was fit. Monovalent affinities (per binding site instead of per antibody were obtained by multiplying dissociation constants by 2 (the number of binding sites per antibody).

ELISAs

The trastuzumab PK kit (Somru Bioscience, Charlottetown, Canada; SB-07-035) was used according to the instructions. Standards were prepared by serially diluting trastuzumab in PBS pH 7.4, 0.1% BSA and subsequently diluting 10-fold in pooled human plasma. Test samples were prepared in a similar way to ensure that they contained 90 % pooled human plasma. To ensure that test samples fell in the linear range of the assay, the 2.3 µM trastuzumab sample was diluted 400-fold in assay buffer, the 1.38 µM test sample was diluted 200-fold, the 500 nM and 138 nM test samples were diluted 100-fold. Calibrators and test samples were then diluted another 50-fold in assay buffer and incubated 1 hour shaking at 300 rpm in 96-well plates coated with anti-therapeutic protein provided with the kit. After three washes with the provided wash buffer, the HRP-conjugated secondary anti-trastuzumab polyclonal antibody was incubated for 1 hour shaking at room temperature. After another three washes, TMB reagent was incubated for 10 minutes at room temperature protected from light. The TMB reaction was stopped by the provided stop solution, turning the product yellow. Absorbance was read out on a Tecan Infinite F500 plate reader at 450 nm with background correction at 620 nm. A 4 parameter curve was fit through the data on a log absorbance/log concentration plot (Fig. S12).

The cetuximab PK kit (Somru Bioscience, Charlottetown, Canada; SBA-100-007-015) was used according to the manufacturer's instructions. Standards were prepared by serially diluting cetuximab in PBS pH 7.4, 0.1% BSA and subsequently diluting 10-fold in pooled human plasma. Test samples were prepared in a similar way to ensure that they contained 90 % pooled human plasma. In accordance with the protocol, a single calibrator series was measured three times. To ensure that test samples fell in the linear range of the assay, the 2.3 µM cetuximab sample was diluted 200-fold in assay buffer, the 500 and 200 nM test samples were diluted 100 fold and the 20 nM sample was diluted 10-fold. Calibrators and test samples were then diluted another 100-fold in assay buffer and incubated 1 hour shaking at 300 rpm in 96-well plates coated with the extracellular domain III of EGFR provided with the kit. After three washes with the provided wash buffer, the HRP-conjugated secondary anti-cetuximab antibody was incubated for 1 hour shaking at room temperature. After another three washes, TMB reagent was incubated for 10 minutes protected from light. The TMB reaction was stopped by the provided stop solution, turning the product yellow. Absorbance was read out on a Tecan Infinite F500 plate reader at 492 nm. A straight line was fit through the data on a Log absorbance / Log concentration plot (equation S1)

$$\log_{10} A = 0.44 \log_{10}[\text{cetuximab}] + 3.03 \qquad \text{Equation S1}$$

The original calibrator concentration was used here. Each test sample was measured six times. For each individual measurement a concentration was calculated using the calibration line and its dilution factor and the mean and SD were calculated from these derived concentrations. Statistics were done in Microsoft Excel. Pearson's R between test samples measured by ELISA and LUMABS was determined by linear regression and statistical significance was determined from the ANOVA test.

Thermodynamic model

The model is schematically shown in Figure 1A in the main text and is an adaptation from a previously published model for a different type of antibody sensor.[4] The equilibrium constants for each step were defined as K_1 for monovalent antibody binding, K_2 for disrupting the helper interaction and K_3 for formation of the bivalent complex. The inverse equilibrium constants (K_1', K_2' and K_3', where $K_1' = 1/K_1$, $K_2' = 1/K_2$ and $K_3' = 1/K_3$) are for the reverse steps. K_1 is solely determined by the monovalent antibody-epitope affinity $K_{\text{d.Ab}}$ and a factor 4 (the number of possible combinations of any of the two antigen binding sites interacting with any of the two epitopes).

$$K_1 = \frac{4}{K_{\text{d.Ab}}} \qquad \text{Equation S2a}$$

K_2 is determined by both the monovalent affinity of this interaction and the effective local concentration of proline rich peptide near the SH3 domain $C_{\text{eff.helper}}$.

$$K_2 = \frac{K_{\text{d.helper}}}{C_{\text{eff.helper}}} \qquad \text{Equation S2b}$$

K_3 is determined by $K_{\text{d.Ab}}$ and the effective local concentration of epitope near the second antigen binding domain $C_{\text{eff.Ab}}$ and a factor 2 (the number of possible states with a single epitope bound to the antibody).

$$K_3 = \frac{C_{\text{eff.Ab}}}{2K_{\text{d.Ab}}} \qquad \text{Equation S2c}$$

The overall apparent dissociation constant of the sensor, $K_{\text{d.app}}$ is the product $K_1' \times K_2' \times K_3'$ (see equation 3 in the main text.) The emission ratio as a function of antibody concentration was defined as the emission ratio of each state S (ER_S) multiplied by the fraction of the sensor that resides in this state, f_S, and then summed over all states. In doing so, the model assumes that the sensor concentration is always much lower than $K_{\text{d.app}}$.

$$ER = \sum_{S=1}^{5}(ER_S f_S) \qquad \text{Equation S3}$$

The numbering of the five different states is indicated in figure 1A in the main text. The fractions f_1, f_2, f_3, f_4 and f_5 are functions of the antibody concentration [Ab]:

$$f_1 = \frac{1}{(1+K_2+K_1[\text{Ab}]+K_1K_2[\text{Ab}]+K_1K_2K_3[\text{Ab}])} \qquad \text{Equation S4a}$$

$$f_2 = \frac{1}{(1+K_2'+K_1[\text{Ab}]+K_1K_2'[\text{Ab}]+K_1K_3[\text{Ab}])} \qquad \text{Equation S4b}$$

$$f_3 = \frac{1}{\left(1+K_2+K_2K_3+\frac{K'_1}{[\mathrm{Ab}]}+\frac{K'_1K_2}{[\mathrm{Ab}]}\right)}$$ Equation S4c

$$f_4 = \frac{1}{\left(1+K'_2+K_3+\frac{K'_1}{[\mathrm{Ab}]}+\frac{K'_1K'_2}{[\mathrm{Ab}]}\right)}$$ Equation S4d

$$f_5 = \frac{1}{\left(1+K'_3+K'_3K'_2+\frac{K'_3K'_1}{[\mathrm{Ab}]}+\frac{K'_3K'_2K'_1}{[\mathrm{Ab}]}\right)}$$ Equation S4e

The dynamic range of the sensor can be written as:

$$DR = \frac{ER_0-ER_\infty}{ER_\infty}$$ Equation S5

The subscripts 0 and ∞ denote the emission ratios at respectively zero and saturating antibody concentrations. The maximally possible dynamic range (under the assumption that the sensor will be completely closed in the absence of antibody and completely in the bivalent state under saturating conditions is:

$$DR_{max} = \frac{ER_1-ER_5}{ER_5}$$ Equation S6

The modelling was done using various values of $K_{d.Ab}$, a fixed value of $K_{d.helper}$ (30 µM) based on literature.[5] $ER_{1,3}$ was fixed at 1.2, based on the 520 nm / 450 nm emission ratio of a previous LUMABS sensor with high affinity HIV1p17 epitopes in the absence of antibody. $ER_{2,4}$ and ER_E were fixed at respectively 0.3 and 0.2, based on the same sensor without helper domains with (ER_E) and without ($ER_{B,D}$) antibody.[2] For modeling the effect of $C_{eff.helper}$ / $C_{eff.Ab}$ on DR / DR_{max} vs. $K_{d.app}$ (Supplementary Figure S1) both local concentrations were first set at 1 mM. $C_{eff.helper}$ was then multiplied by the square root of a varying number (indicated in the legend) while $C_{eff.Ab}$ was divided by the square root of the same number. For each ratio, $K_{d.Ab}$ was then varied from 10 nM to 86 µM. $K_{d.app}$ was calculated using equation 3 and DR / DR_{max} was calculated using equations S5 and S6. Curves in Figure 1B in the main text were generated with a ratio of 10, meaning that $C_{eff.helper}$ was $\sqrt{10}$ mM and $C_{eff.Ab}$ was 1 / $\sqrt{10}$ mM. This was in good agreement with the experimental curves. It is difficult to predict these concentrations precisely, but the estimate is reasonable, given that Intramolecular interaction partners are known to have effective local concentrations in the high micromolar to low millimolar range[6,7] and that flexible linkers span shorter distances far more readily than longer ones.

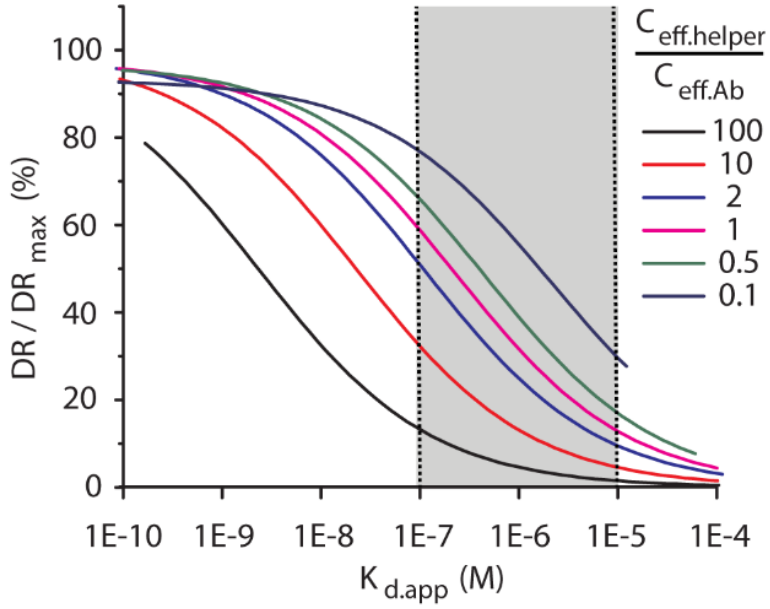

Supplementary Figure S1. Plots of DR / DR_{max} vs. $K_{d.app}$ for different $C_{eff.helper}$ / $C_{eff.Ab}$. Both effective concentrations were first set at 1 mM. Then, $C_{eff.helper}$ was multiplied by the square root of the ratio indicated in the legend, while $C_{eff.Ab}$ was divided by the same ratio. For example, a ratio of 10 means $C_{eff.helper}$ is $\sqrt{10}$ mM and $C_{eff.Ab}$ is $1/\sqrt{10}$ mM. For each ratio, $K_{d.app}$ and DR / DR_{max} were calculated with varying $K_{d.Ab}$ values ranging from 10 nM to 86 µM using equations 3, S5 and S6. These are shown on the horizontal and vertical axis respectively. The decline in dynamic range occurs at higher $K_{d.app}$ for lower $C_{eff.helper}$ / $C_{eff.Ab}$ ratios. However, when the ratio is very low (e.g. 0.1), another effect is seen, namely that the sensor does not fully close even in the absence of antibody.

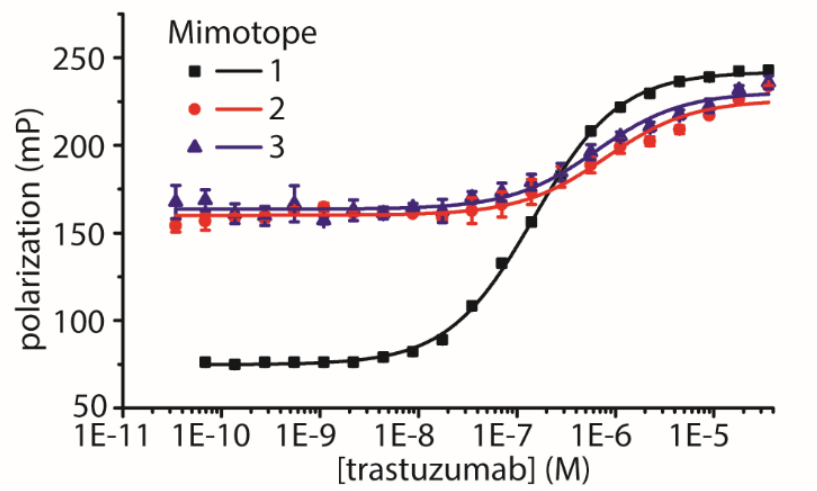

Supplementary Figure S2. Trastuzumab binding to mimotopes 1, 2 and 3. Trastuzumab was titrated to 30 nM FITC-labeled mimotope peptide in a total volume of 10 µL PBS pH 7.4 with 0.1 % BSA. Data represent mean ± SD from three experiments. K_d values obtained from fitting one-site binding models through the data, multiplied by 2 (the number of independent binding sites on the antibody) are provided in Table 1 in the main text.

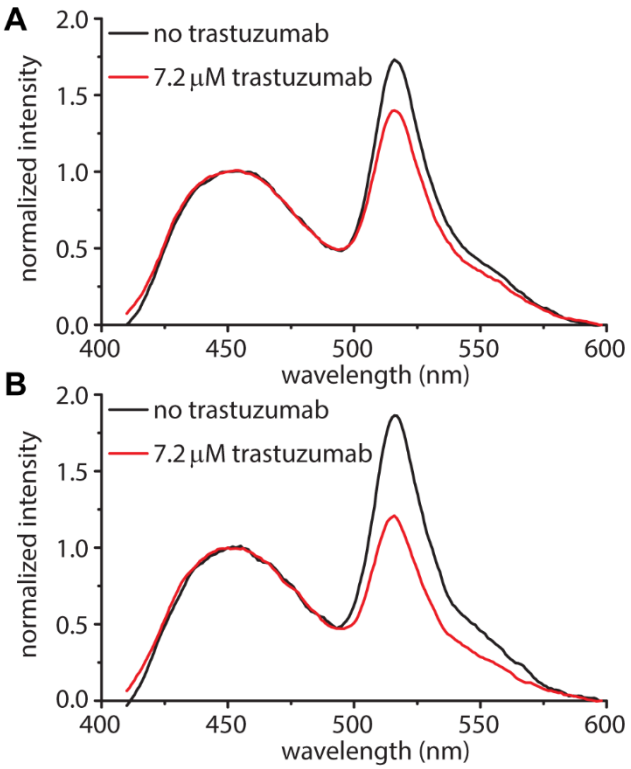

Supplementary Figure S3. Luminescence emission spectra of trastuzumab sensors. Spectra of TRAS-LUMABS-2 (A) and 3 (B) were recorded using 100 pM sensor in PBS pH 7.4 with 0.1 % BSA and a NanoGlo dilution of 1000-fold with or without trastuzumab.

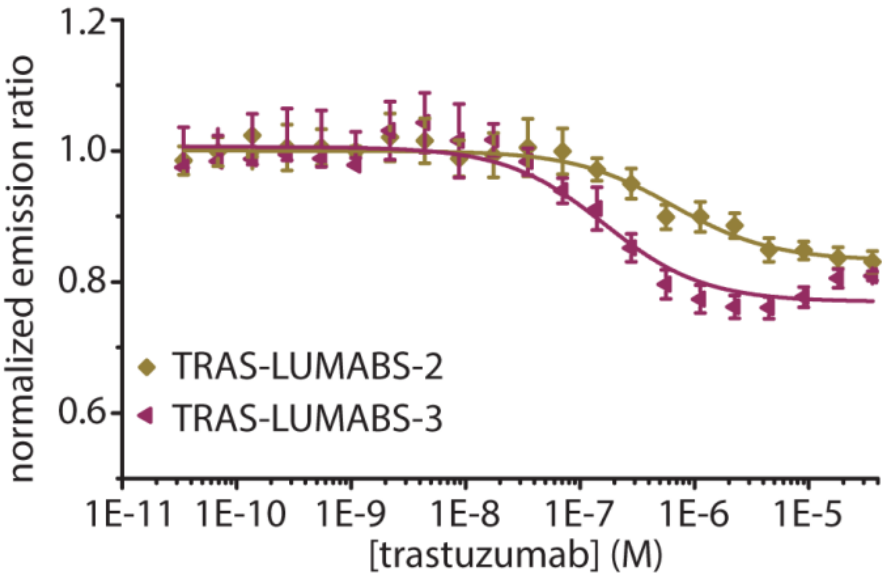

Supplementary Figure S4. Trastuzumab titrations to 100 pM of TRAS-LUMABS-2 or 3 in PBS pH 7.4 with 0.1 % BSA and a NanoGlo dilution of 1000-fold.. Data represent mean ± SD from triplicate measurements.

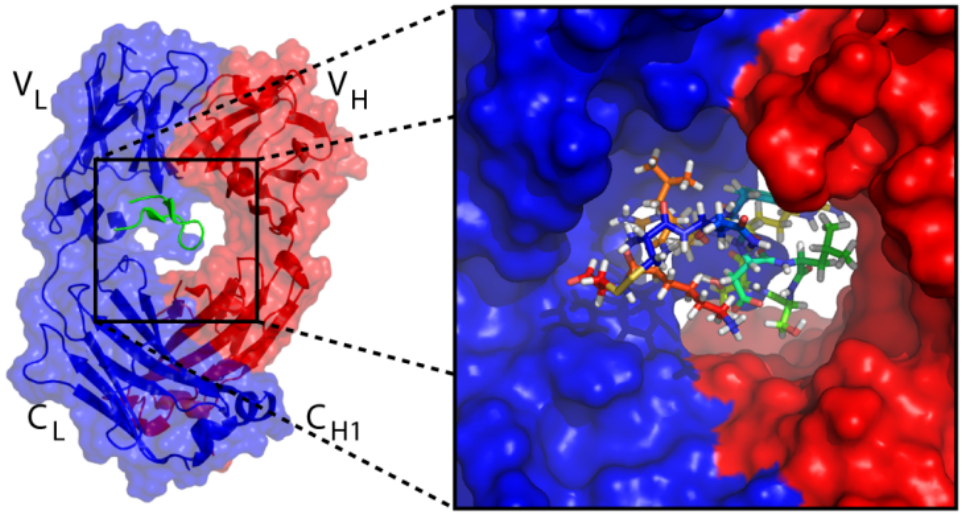

Supplementary Figure S5. Structure of the meditope peptide used in CTX-LUMABS-1 in complex with the cetuximab Fab fragment (PDB: 4GWL)[12]. Heavy chains are colored in red, light chains in blue and the meditope in green. The insert shows the meditope peptide in a rainbow-pattern from N-to C-terminus and the antibody as a surface representation.

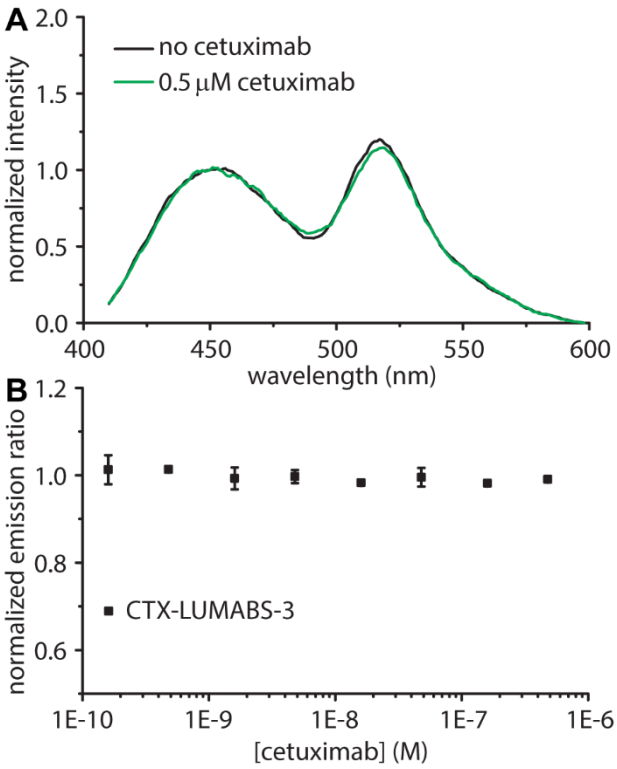

Supplementary Figure S6. Cyclization of CTX-LUMABS sensor is required for its function. A) Luminescence emission spectra of 100 pM sensor protein CTX-LUMABS-3 in 200 µL PBS pH 7.4 with 0.1 % BSA with the indicated concentration of cetuximab and a NanoGlo substrate dilution of 1000x. B) Spectra like those in (A) were recorded at different cetuximab concentrations, from which green/blue emission ratios were calculated. Data represent mean ± SEM from two measurements. Data were normalized to the average emission ratio across all measurements.

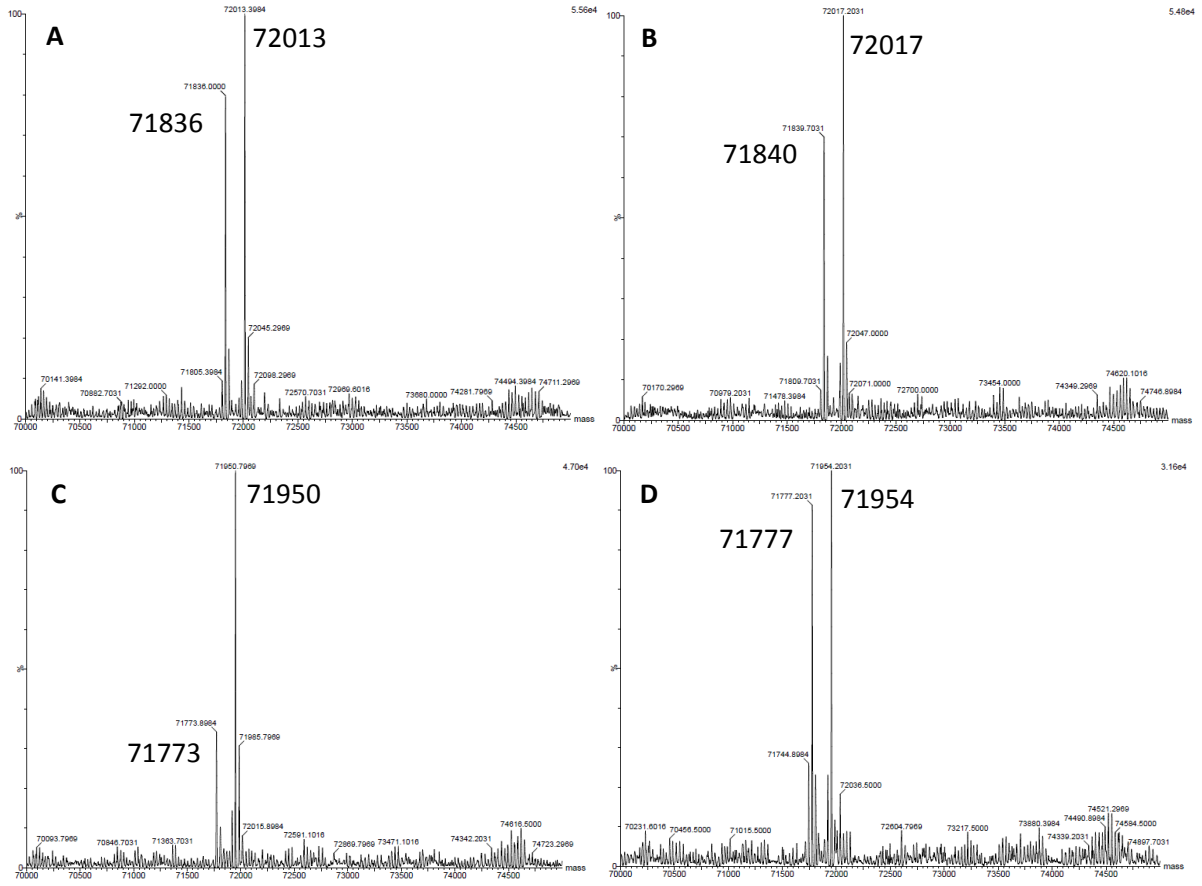

Supplementary Figure S7. Mass spectra of CTX-LUMABS-1 and -2 determined by QTof-MS. (A) CTX-LUMABS-1 (calculated mass with two disulfide-bonds formed and lacking the N-terminal methionine: 71838 Da) (B) DTT-reduced CTX-LUMABS-1; (C) CTX-LUMABS-2 (calculated mass with two disulfide-bonds formed and lacking the N-terminal methionine: 71774 Da); (D) DTT-reduced CTX-LUMABS-2. The Δ177 Da masses observed for all samples are attributed to α-N-6-phospho-gluconoylation of the N-terminal His-tag.

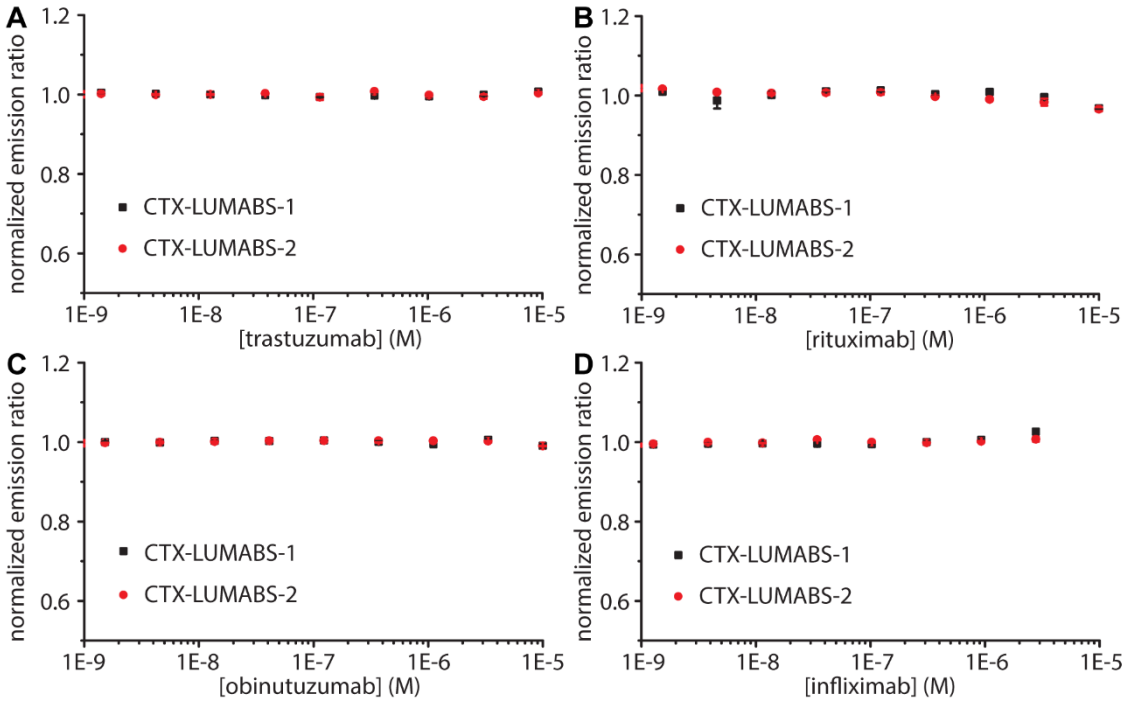

Supplementary Figure S8. Specificity of cetuximab-LUMABS sensors. Antibodies trastuzumab (A), rituximab (B), obinutuzumab (C) and infliximab (D) were titrated to 100 pM CTX-LUMABS-1 and CTX-LUMABS-2 in PBS pH 7.4 with 0.1 % BSA with a NanoGlo substrate dilution of 1000x. Data represent mean ± SD from duplicate experiments.

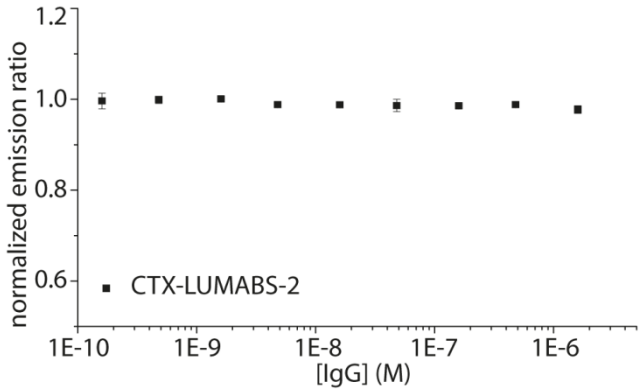

Supplementary Figure S9. Titration of IgG to CTX-LUMABS-2. Spectra of 100 pM CTX-LUMABS-2 in 200 µL PBS pH 7.4 with 0.1 % BSA with a NanoGlo substrate dilution of 1000× were recorded at different concentrations of IgG, from which green / blue emission ratios were calculated. Data represent mean ± SEM from two measurements. Data were normalized to the average emission ratio across all measurements.

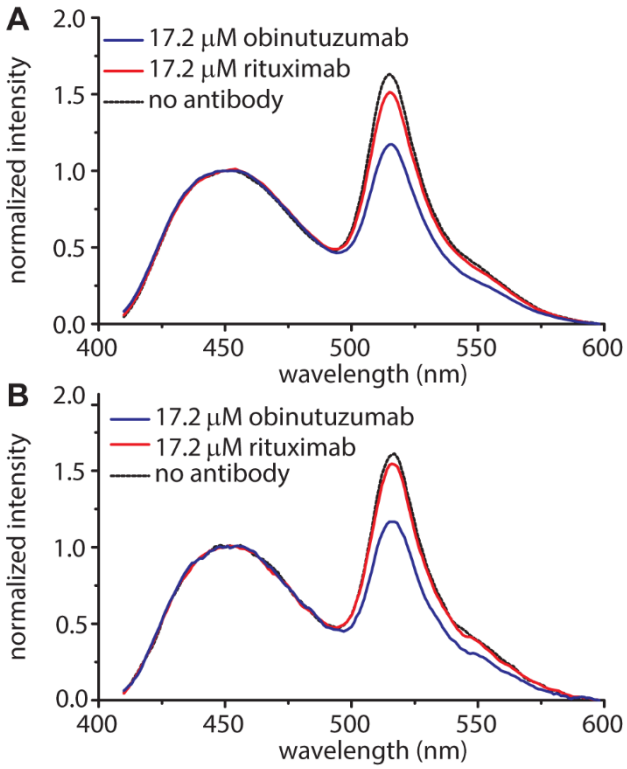

Supplementary Figure S10. Luminescence emission spectra of anti-CD20 antibody sensors. Spectra of CD20-LUMABS-1 (A) and 2 (B) were recorded at 100 pM sensor in PBS pH 7.4 with 0.1 % BSA and a NanoGlo dilution of 1000-fold with or without obinutuzumab or rituximab.

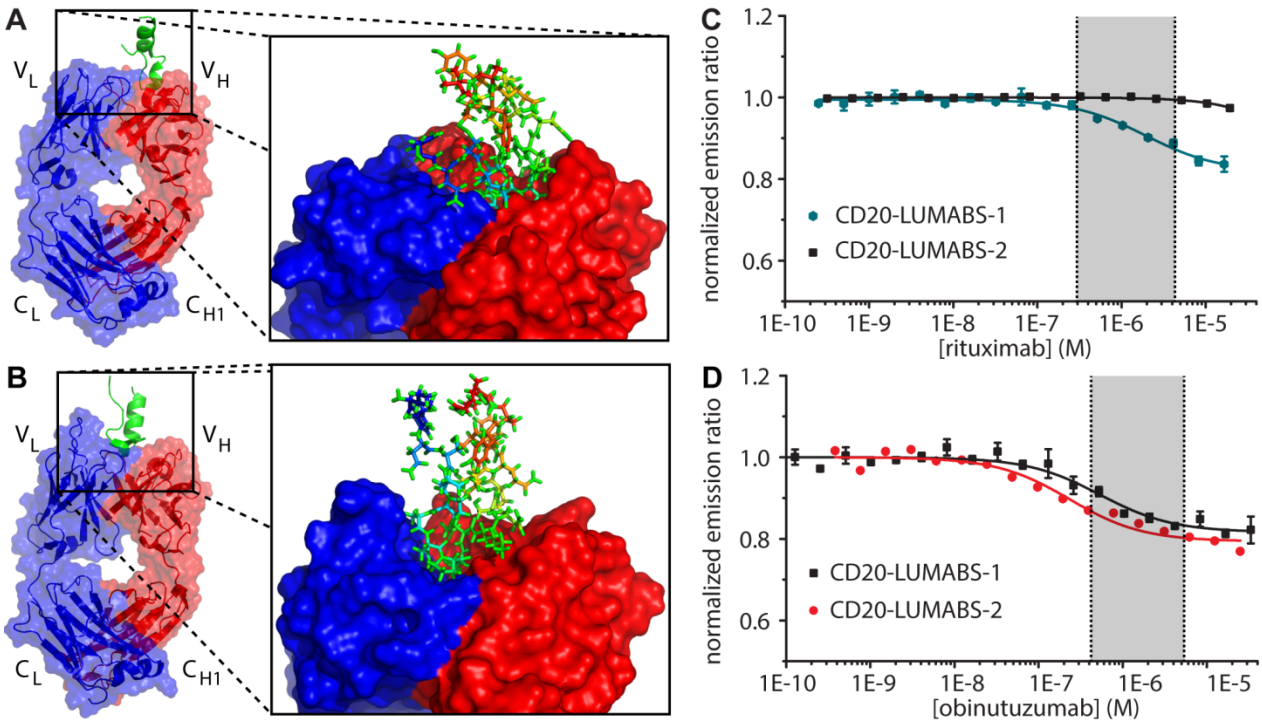

Supplementary Figure S11. Characterization of LUMABS sensors for anti CD20 antibodies. A, B) Structures of the cyclic CD20 epitope peptide used in CD20-LUMABS-1 in complex with (A) rituximab (PDB: 3PP4)[8] or (B) obinutuzumab (PDB: 2OSL)[9] Fab fragments. Heavy chains are colored in red, light chains in blue and the epitope in green. Inserts show the epitope peptide in a rainbow-pattern from N-to C-terminus and the antibodies as surface representations. Images were generated using PyMol. C, D) rituximab (C) and obinutuzumab (D) titrations to 100 pM CD20-LUMABS 1 and 2. Data represent mean ± SD from three measurements. The shaded area represents the clinically relevant concentration range from data in ref.[10] (C) or [11] (D).

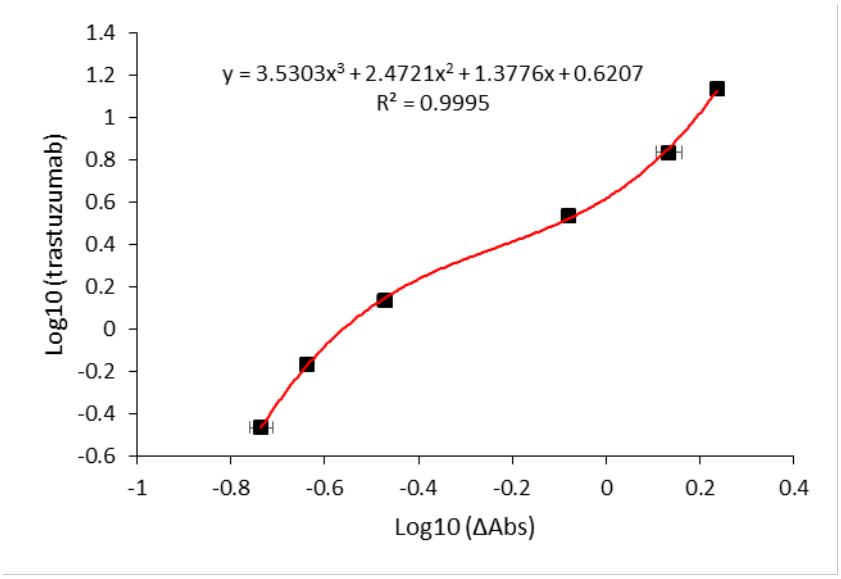

Supplementary Figure S12. Calibration of commercial tratuzumab ELISA. The data represent mean ± SD of triplicate measurements. The calibration curve with the indicated formula in the figure was used to calculate concentrations from absorbance values in the test samples in Figure 4 in the main text.

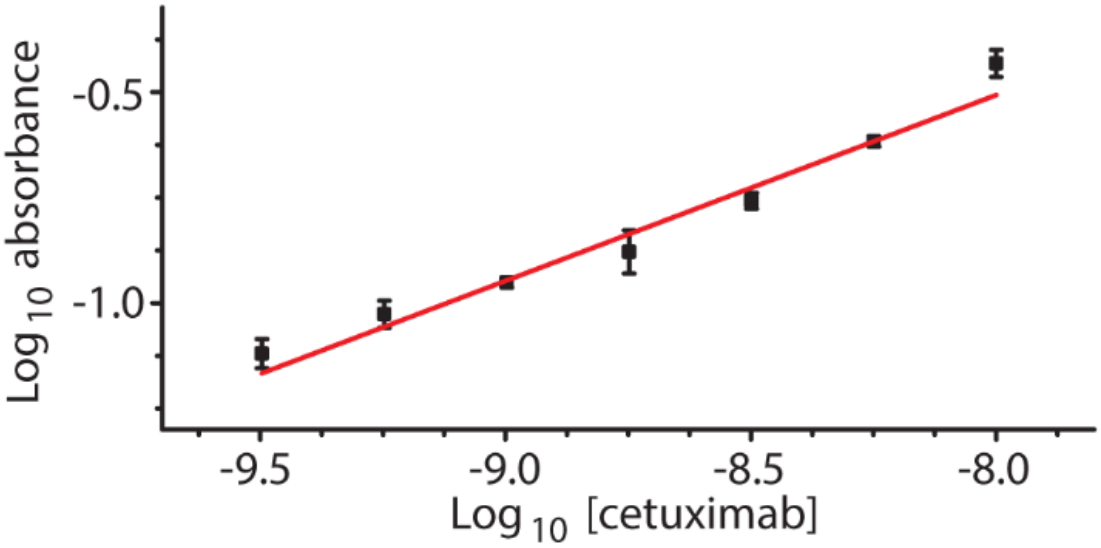

Supplementary Figure S13. Calibration of commercial cetuximab ELISA. The data represent mean ± SD from triplicate measurements of a single series of calibrators. A straight line was fit through the data (see equation S1 of the Supplementary Experimental Procedures).

TRAS-LUMABS-1

```
atgggcagcagccatcatcatcatcatcacagcagcggcctggtgccgcgcggcagccatatggctagcgacgacaacttt
 M  G  S  S  H  H  H  H  H  H  S  S  G  L  V  P  R  G  S  H  M  A  S  D  D  N  F
atatacaaggcgaaggcgctctatccctatgatgcagatgatgatgacgcatacgaaatctcattcgaacaaaatgaaatc
 I  Y  K  A  K  A  L  Y  P  Y  D  A  D  D  D  D  A  Y  E  I  S  F  E  Q  N  E  I
cttcaggtatcagacattgaggggcggtggtggaaagcccgccgcgccaatggagagacaggcatcatcccgtcgaattat
 L  Q  V  S  D  I  E  G  R  W  W  K  A  R  R  A  N  G  E  T  G  I  I  P  S  N  Y
gttcagttgattgacggtcctgaggaaatgcatcgggggcggctcgggaggctcaggcagccatatggtaagtaaaggtgaa
 V  Q  L  I  D  G  P  E  E  M  H  R  G  G  S  G  G  S  G  S  H  M  V  S  K  G  E
gaagacaatatggcttctctgcctgccacacatgagcttcatattttgggagcataaacggagtggatttcgacatggta
 E  D  N  M  A  S  L  P  A  T  H  E  L  H  I  F  G  S  I  N  G  V  D  F  D  M  V
ggtcagggtacggggaaccctaacgatggatatgaggagttgaatcttaaaagcacaaagggtgatctgcagttctcgccc
 G  Q  G  T  G  N  P  N  D  G  Y  E  E  L  N  L  K  S  T  K  G  D  L  Q  F  S  P
tggatcctggtgccgcatataggttatggtttccatcagtatcttccatacccggatggcatgagccctttcaggccgca
 W  I  L  V  P  H  I  G  Y  G  F  H  Q  Y  L  P  Y  P  D  G  M  S  P  F  Q  A  A
atggtagatggctcaggatatcaagtgcatcggaccatgcagtttgaagatggggcgtctttgacggtaaattacaggtac
 M  V  D  G  S  G  Y  Q  V  H  R  T  M  Q  F  E  D  G  A  S  L  T  V  N  Y  R  Y
acctatgagggtagccatataaagggagaagcgcaggtgaagggaactggattcccagcggatggcccagtcatgacaaac
 T  Y  E  G  S  H  I  K  G  E  A  Q  V  K  G  T  G  F  P  A  D  G  P  V  M  T  N
agcctcaccgctgctgattggtgccgatccaagaaaacgtatccaaacgataaaactatcatttctacttttaagtggtcc
 S  L  T  A  A  D  W  C  R  S  K  K  T  Y  P  N  D  K  T  I  I  S  T  F  K  W  S
tatacaacaggaaacgggaaacgctatcgttcaacggcccgcacgacctacacgtttgcaaagccaatggctgcgaattat
 Y  T  T  G  N  G  K  R  Y  R  S  T  A  R  T  T  Y  T  F  A  K  P  M  A  A  N  Y
ctgaaaaaccagccgatgtatgtgttccgtaaaaccgaactgaaacattctaaaacggagctcaatttcaaggaatggcag
 L  K  N  Q  P  M  Y  V  F  R  K  T  E  L  K  H  S  K  T  E  L  N  F  K  E  W  Q
aaggcatttacggatgtcatgggaatggacgaactgtataagtcgggcggaggtacccagctgggcccgtatgaactgtgg
 K  A  F  T  D  V  M  G  M  D  E  L  Y  K  S  G  G  G  T  Q  L  G  P  Y  E  L  W
gaactgagccatgggggttcgggtggttcaggcggctcaggaggctccgggggttccggagggagcggtgctgaagccgca
 E  L  S  H  G  G  S  G  G  S  G  G  S  G  G  S  G  G  S  G  G  S  G  A  E  A  A
gccaaggaagcagcagctaaagaggccgctgcgaaggaagctgccgcaaaggaggcggcggcgaaagaggcggcagcaaaa
 A  K  E  A  A  A  K  E  A  A  A  K  E  A  A  A  K  E  A  A  A  K  E  A  A  A  K
gccggatctggtggcagtggtggctccggcgggtcaggtggcagcgggggatcaggagctgaggcagccgccaaagaggct
 A  G  S  G  G  S  G  G  S  G  G  S  G  G  S  G  G  S  G  A  E  A  A  A  K  E  A
gcggccaaggaggccgccgctaaagaagccgcggcaaaagaggcagcggcaaaggaagcggctgcgaaagccggaagtggt
 A  A  K  E  A  A  A  K  E  A  A  A  K  E  A  A  A  K  E  A  A  A  K  A  G  S  G
gggtcgggcggctccggtggctctggcggcagtggcggtagtggcgggcaattagggccatacgagttatgggagttatca
 G  S  G  G  S  G  G  S  G  G  S  G  G  S  G  G  Q  L  G  P  Y  E  L  W  E  L  S
cacactagtggaggcagcatggtatttactcttgaagattttgtcggtgattggcgccagaccgccggctataacctggac
 H  T  S  G  G  S  M  V  F  T  L  E  D  F  V  G  D  W  R  Q  T  A  G  Y  N  L  D
caagtgcttgaacagggcggggttagcagcctgtttcaaaacctgggggtgagtgtcacgccaattcagcgcatcgttctg
 Q  V  L  E  Q  G  G  V  S  S  L  F  Q  N  L  G  V  S  V  T  P  I  Q  R  I  V  L
tcgggagagaatggtctgaaaatcgatatccacgtcattatcccgtacgaaggtctttctggtgatcagatggggcagata
 S  G  E  N  G  L  K  I  D  I  H  V  I  I  P  Y  E  G  L  S  G  D  Q  M  G  Q  I
gaaaaaatattcaaagtggtgtacccagtagacgatcatcacttcaaggttatactgcactatggcaccctcgttatcgat
 E  K  I  F  K  V  V  Y  P  V  D  D  H  H  F  K  V  I  L  H  Y  G  T  L  V  I  D
ggcgttactccgaatatgatcgattactttgggcgtccttatgaaggtattgcggtgttcgacggtaaaaaaattacggtt
 G  V  T  P  N  M  I  D  Y  F  G  R  P  Y  E  G  I  A  V  F  D  G  K  K  I  T  V
accgggacgctctggaatggtaataaaatcattgatgagcgcttgataaacccagatggcagccttctgttcagagttacg
 T  G  T  L  W  N  G  N  K  I  I  D  E  R  L  I  N  P  D  G  S  L  L  F  R  V  T
ataaacggggttacgggttggcgactgtgcgaaagaatattagcttctagcggtggaggatctattcgttcaaagccgctg
 I  N  G  V  T  G  W  R  L  C  E  R  I  L  A  S  S  G  G  G  S  I  R  S  K  P  L
ccacccctacccgtgtaatag
 P  P  L  P  V  -  -
```

SH3 domain | mNeonGreen | N-terminal mimotope
C-terminal mimotope | NanoLuc | proline-rich peptide

Supplementary Figure S14 Sequence of TRAS-LUMABS-1

TRAS-LUMABS-2 (mimotopes only)

```
N-terminal: ctgtggggcccgtatgagtggtgggaactgcatcac
             L  W  G  P  Y  E  W  W  E  L  H  H
C-terminal: ttatggggtccttacgaatggtgggagctgcaccat
             L  W  G  P  Y  E  W  W  E  L  H  H
```

TRAS-LUMABS-3 (mimotopes only)

```
N-terminal: ctgtggggcccgtatgagtggtgggaatttcatcac
             L  W  G  P  Y  E  W  W  E  F  H  H
C-terminal: ttatggggtccttacgaatggtgggagtttcaccat
             L  W  G  P  Y  E  W  W  E  F  H  H
```

CTX-LUMABS-1 (meditopes only)

```
N-terminal: tgtcagtttgacttaagcacccgtcgcctgaaatgc
             C  Q  F  D  L  S  T  R  R  L  K  C
C-terminal: tgccaattcgatctgagtacgcgccgtttaaagtgt
             C  Q  F  D  L  S  T  R  R  L  K  C
```

CTX-LUMABS-2 (meditopes only)

```
N-terminal: tgtgtgtttgacttaggcacccgtcgcctgcgttgc
             C  V  F  D  L  G  T  R  R  L  R  C
C-terminal: tgcgttttcgatctgggtacgcgccgtttacgctgt
             C  V  F  D  L  G  T  R  R  L  R  C
```

CTX-LUMABS-3 (meditopes only)

```
N-terminal: gcggtgtttgacttaggcacccgtcgcctgcgtgcc
             A  V  F  D  L  G  T  R  R  L  R  A
C-terminal: gcggttttcgatctgggtacgcgccgtttacgcgcc
             A  V  F  D  L  G  T  R  R  L  R  A
```

CD20-LUMABS-1 (epitopes only)

```
N-terminal: tacaattgtgaaccagcgaatccgtctgagaaaaacagccctagtacccaatattgctacagcatc
             Y  N  C  E  P  A  N  P  S  E  K  N  S  P  S  T  Q  Y  C  Y  S  I
C-terminal: tataactgcgagccggccaaccctagcgaaaagaattctccgagcacacagtactgttattctatt
             Y  N  C  E  P  A  N  P  S  E  K  N  S  P  S  T  Q  Y  C  Y  S  I
```

CD20-LUMABS-2 (epitopes only)

```
N-terminal: tacaattgtgcaccagcgactccgtctgagaaaaacagccctagtacccaatattgctacagcatc
             Y  N  C  A  P  A  T  P  S  E  K  N  S  P  S  T  Q  Y  C  Y  S  I
C-terminal: tataactgcgcgccggccacccctagcgaaaagaattctccgagcacacagtactgttattctatt
             Y  N  C  A  P  A  T  P  S  E  K  N  S  P  S  T  Q  Y  C  Y  S  I
```

Supplementary Figure S15. Sequences of epitopes, mimotopes and meditopes incorporated in LUMABS proteins used in this study.

Supplementary References

(1) Liu, H.; Naismith, J. H. *BMC Biotechnol.* **2008**, *8*, 91.

(2) Arts, R.; Den Hartog, I.; Zijlema, S. E.; Thijssen, V.; Van Der Beelen, S. H. E.; Merkx, M. *Anal. Chem.* **2016**, *88* , 4525–4532.

(3) van Rosmalen, M.; Janssen, B. M. G.; Hendrikse, N. M.; van der Linden, A. J.; Pieters, P. A.; Wanders, D.; de Greef, T. F. A.; Merkx, M. *J. Biol. Chem.* **2017**, *292*, 1477-1489

(4) Banala, S.; Aper, S. J. A.; Schalk, W.; Merkx, M. *ACS Chem. Biol.* **2013**, *8* , 2127–2132.

(5) Grünberg, R.; Burnier, J. V.; Ferrar, T.; Beltran-Sastre, V.; Stricher, F.; Van Der Sloot, A. M.; Garcia-Olivas, R.; Mallabiabarrena, A.; Sanjuan, X.; Zimmermann, T.; Serrano, L. *Nat. Methods* **2013**, *10*, 1021–1027.

(6) Krishnamurthy, V. M.; Semetey, V.; Bracher, P. J.; Shen, N.; Whitesides, G. M. *J. Am. Chem. Soc.* **2007**, *129*, 1312–1320.

(7) Sethi, A.; Goldstein, B.; Gnanakaran, S. *PLOS Comput. Biol.* **2011**, *7*, e1002192.

(8) Niederfellner, G.; Lammens, A.; Mundigl, O.; Georges, G. J.; Schaefer, W.; Schwaiger, M.; Franke, A.; Wiechmann, K.; Jenewein, S.; Slootstra, J. W.; Timmerman, P.; Brännström, A.; Lindstrom, F.; Mössner, E.; Umana, P.; Hopfner, K.-P.; Klein, C. *Blood* **2011**, *118*, 358–367.

(9) Du, J.; Wang, H.; Zhong, C.; Peng, B.; Zhang, M.; Li, B.; Huo, S.; Guo, Y.; Ding, J. *J. Biol. Chem.* **2007**, *282*, 15073–15080.

(10) Berinstein, N. L.; Grillo-López, A. J.; White, C. A.; Bence-Bruckler, I.; Maloney, D.; Czuczman, M.; Green, D.; Rosenberg, J.; McLaughlin, P.; Shen, D. *Ann. Oncol.* **1998**, *9*, 995–1001.

(11) Cartron, G.; Hourcade-Potelleret, F.; Morschhauser, F.; Salles, G.; Wenger, M.; Truppel-Hartmann, A.; Carlile, D. J. *Haematologica* **2016**, *101*, 226–234.

(12) Donaldson, J. M.; Zer, C.; Avery, K. N.; Bzymek, K. P.; Horne, D. A.; Williams, J. C. *Proc. Natl. Acad. Sci. U. S. A.* **2013**, *110*, 17456–17461.